

Modeling the water scrubbing process and energy requirements for CO_2 capture to upgrade biogas to biomethane

William J. Nock,^{*,†} Mark Walker,[‡] Rimika Kapoor,[¶] and Sonia Heaven[†]

Faculty of Engineering and the Environment, University of Southampton, Highfield, Southampton, SO17 1BJ, United Kingdom, Energy Technology Innovation Initiative, University of Leeds, Woodhouse Lane, Leeds, LS2 9JT, United Kingdom, and Centre for Rural Development and Technology, Foundation for Innovation and Technology Transfer, Indian Institute of Technology Delhi, Haus Khaz, New Delhi, 110 016, India

E-mail: w.j.nock@soton.ac.uk

Phone: +44 (0)23 8059 5000. Fax: +44 (0)23 8059 3131

This document is the unedited author's version of a Submitted Work that was subsequently accepted for publication in Industrial Engineering & Chemistry Research, copyright American Chemical Society after peer review. To access the final edited and published work, see <http://pubs.acs.org/doi/abs/10.1021/ie501280p>

*To whom correspondence should be addressed

†University of Southampton

‡University of Leeds

¶Indian Institute of Technology Delhi

Abstract

Water scrubbing is the most widely used technology for removing CO_2 from biogas and landfill gas. This work developed a rate-based mass transfer model of the CO_2 -water system for upgrading biogas in a packed bed absorption column. The simulated results showed good agreement with both a pilot-scale plant operating at 10 bar, and a large-scale biogas upgrading plant operating at atmospheric pressure. The calculated energy requirement for the absorption column to upgrade biogas to 98% CH_4 (0.23 kWh Nm^{-3} , or 4.2 % of the input biogas) is a significantly closer approximation to the measured value (0.26 kWh Nm^{-3} , or 4.8 % of the input biogas) than has previously been reported in the literature. The model allows for improved design of CO_2 capture and biogas upgrading operations, and can also be a useful tool for more detailed cost-benefit analysis of the technology.

Nomenclature

a	Interfacial area	$m^2 \text{ m}^{-3}$
A	Cross sectional area	m^2
a_p	Packing surface area	$m^2 \text{ m}^{-3}$
a_w	Wetted surface area	$m^2 \text{ m}^{-3}$
C_G	Gas phase constant	
C_L	Liquid phase constant	
C_{PK}	Packing specific constant	
c	Molar concentration	mol m^{-3}
d_H	Hydraulic diameter	m
d_p	Particle diameter (defined as $6(1 - \epsilon)/a_p$)	m
D	Diffusion coefficient	$m^2 \text{ s}^{-1}$
g	Acceleration of gravity	$m \text{ s}^{-2}$
G	Superficial mass velocity of gas	$kg \text{ m}^{-2} \text{ s}^{-1}$

h	hold-up	$m^3 m^{-3}$
H	Liquid head	m
H_G	Henry's Constant	kPa
k	Mass transfer coefficient	s^{-1}
K	Overall mass transfer coefficient	s^{-1}
L	Superficial mass velocity of liquid	$kg m^{-2} s^{-1}$
n	Number of compression stages	
N	Mass transfer flux	$mol s^{-1}$
P	Power	kW
p	Pressure	kPa
Q	Flow rate	$m^3 s^{-1}$
R	Gas constant	$J K^{-1} mol^{-1}$
t	time	s
T	Temperature	K
u	Superficial velocity	$m s^{-1}$
y	Gaseous mole fraction	
z	Column height	

Dimensionless Numbers

Fr_L	Froude number	$\frac{a_p L^2}{g \rho_L^2}$
Sc	Schmidt number	$\frac{\nu}{D}$
Re_L	Reynolds number	$\frac{\rho_L u_L d_H}{\mu_L}$
	or	$\frac{\rho_L u_L}{a_w \mu_L}$
We_L	Weber number	$\frac{L^2}{\rho_L \sigma_L a_p}$

Greek Letters

ϵ	Void fraction	$(m^3 m^{-3})$
η	Efficiency	
μ	Dynamic viscosity	$(kg m^{-1} s^{-1})$
ν	Kinematic viscosity	$(m^2 s^{-1})$
ρ	Density	$(kg m^{-3})$
σ	Surface tension	$(kg s^{-1})$
σ_c	Critical surface tension of packing material	$(kg s^{-1})$
ξ	Performance index	
γ	Specific heat	
Φ	Enhancement factor for turbulent diffusion	
ϕ_p	Form factor	

Subscripts (where otherwise not defined)

1	Input
2	Output
<i>ATM</i>	Atmospheric pressure head
<i>C</i>	Compressor
<i>COL</i>	Column pressure head
<i>COOL</i>	Coolant
<i>D</i>	Dynamic pressure head
<i>e</i>	Enriched biogas (from equation 10)
<i>eq</i>	Concentration in equilibrium with partial pressure
<i>G</i>	Gas phase
<i>L</i>	Liquid phase\Liquid pumping
<i>mol</i>	Molar
<i>P</i>	Pump
<i>r</i>	Raw biogas (from equation 10)
<i>S</i>	Static pressure head
<i>T</i>	Total
<i>w</i>	Water

Introduction

Removal of CO_2 from gas streams is an important process both as a potential step in greenhouse gas sequestration, and for upgrading biogas. Biogas is produced from the anaerobic digestion of organic waste material and is mainly composed of CO_2 (typically 35 - 45 %) and CH_4 (typically 55 - 65 %) with smaller proportions of H_2S , water vapour and other trace compounds. This biogas can be combusted directly on site in a boiler or a combined heat and power (CHP) unit. If the electricity and/or heat produced exceeds on-site requirements, however, an alternative option is to upgrade and export the biogas for use where needed.

The upgrading process produces biomethane, with comparable properties to natural gas, and involves removal of the non-combustible fractions to increase the calorific value of the gas. This can enable the upgraded biogas to meet the standards for injection into a natural gas grid, or for use as a vehicle fuel replacing compressed natural gas (CNG). This is a particularly attractive option in situations where there is insufficient local demand for the heat produced from a CHP plant, making upgrading the most efficient option in terms of overall energy balance.¹

Several countries have set their own biomethane standards for use in the gas grid or as a vehicle fuel. Switzerland and Sweden require a 96% and 97 % CH_4 content, respectively.² The European Committee for Standardisation is currently working to produce a European standard on biomethane. Typically a CH_4 concentration of over 95 % is required for vehicle or gas grid use. To achieve this a significant portion of CO_2 from biogas needs to be removed. Different methods are currently employed to achieve this, including pressure swing adsorption, cryogenic, chemical absorption and membrane techniques.³ Currently the most widely-used method in the biogas industry is the water absorption process.⁴ This procedure mixes water and biogas, counter-currently, usually under pressure in a packed column to maximise the gas-liquid contact area. CO_2 is more readily absorbed in water than CH_4 , so in the absorption column more of the CO_2 is removed from the gas stream, increasing the CH_4 concentration in the biogas. At 273 K CO_2 has a molar concentration approximately 29 times greater than CH_4 , although this ratio reduces with temperature to approximately 23:1 at 303°K. The solubilities of both CO_2 and CH_4 increase with a reduction in temperature.

Depending on the substrate and operating conditions used in the anaerobic digestion process, other compounds such as H_2S and N_2 may be present in the biogas; and some of these may need to be removed before or during CO_2 removal. An advantage of the water absorption

process is that it can also be used to remove low concentrations of H_2S .⁴ Difficulties can arise, however, if a desorption step is employed to regenerate the water for recirculation back into the absorption column. The desorption step requires mixing with air, and high concentrations of H_2S will oxidise into H_2SO_4 , which can lead to corrosion problems. In this case a pre-treatment step can remove H_2S prior to upgrading. For the purposes of this model only CH_4 and CO_2 have been considered and the presence of H_2S has been assumed to be negligible.

There is a lack of published work investigating the energy requirements of the CO_2 water scrubbing process. A life cycle assessment from Berglund and Börjesson⁵ on the anaerobic digestion of different feedstocks included an energy analysis of biogas upgrading. It was estimated that 11 % of the energy content of the produced biogas is used to meet the energy demands of the upgrading process, although no reference is made to the type of process used. Smyth et al.⁶ investigated the energy balance of biomethane from anaerobic digestion of grasses, and used a range of 0.3 - 0.6 $kWh Nm^{-3}$ for the energy requirement of gas scrubbing; but no further detail on the scrubbing process is included. A life cycle assessment from Jury et al.⁷ provides more detail, estimating 3 % of the energy content in the upgraded biogas is required when the water scrubbing process is operated at 8 bar. The Swedish Gas Centre conducted reviews of operational biogas upgrading plants in 2003⁸ and 2013.⁴ The original study from Persson⁸ found the energy consumption for water scrubbing plants was between 0.3 – 0.6 $kWh Nm^{-3}$ (output biomethane), corresponding to 3 – 6 % of the energy content of the upgraded biomethane. The more recent study from Bauer et al.⁴ compared the energy requirements of the different biogas upgrading techniques. It found that water scrubbing had similar energy requirements to the pressure swing adsorption method, requiring approximately 0.2 – 0.3 $kWh Nm^{-3}$ (input biogas). The literature values show some disagreement, with many of the reported values quoted in different terms and under different operational conditions. This work aimed to model the absorption column used in the water

scrubbing procedure to allow detailed analysis of the energy requirements of the process under different operational conditions.

Optimisation of the biogas upgrading process is necessary to reduce the energy consumption and operational costs of the upgrading plant. Over the last few decades there has been extensive research on gas liquid mass transfer in packed beds. Dozens of correlations for the mass transfer coefficient have been proposed for these and similar systems. A recent review and comparison of the mass transfer coefficients for random and structured packings is given by Wang et al.⁹

There has also been much work on the hydrodynamics of packed bed columns, with studies by Hiby¹⁰ and more recently Therning and Rasmuson¹¹ who conducted experiments showing the poor radial mixing and inaccuracy of the axial dispersion model to describe packed bed reactors.

Recently published studies modeling biogas upgrading, such as Gabrielsen et al.,¹² have focused on chemical absorption techniques. There is also interest in this technique for the removal of CO_2 from flue gas (Yeh et al.¹³ and Rao and Rubin¹⁴). Experimental investigations on the efficiency of the water absorption process for upgrading landfill gas were conducted by Rasi et al.¹⁵ This work compared different operational pressures as well as gas and liquid flow rates in the absorption column. There is currently a lack of reported studies, however, on modeling of the water absorption technique for the scrubbing of CO_2 from flue gas or biogas.

Methodology

Mass Transfer Model

A mass transfer rate-based model was developed to calculate the mass transfer of CO_2 and CH_4 from biogas into water in a packed bed absorption column. This model uses a one dimensional finite difference approach to calculate the concentration at different points along the column. Figure 1 shows a representation of the counter-current finite difference approximation used, over a difference in column height Δz . The flow rates are in terms of the biogas (Q_G) and water (Q_L). While the concentrations are divided into the gaseous and aqueous concentrations of CO_2 and CH_4 , shown by $[CO_{2(G)}]$, $[CO_{2(AQ)}]$ and $[CH_{4(G)}]$, $[CH_{4(AQ)}]$, respectively. Similarly the mass transfer for CO_2 and CH_4 in the gas and liquid phases were calculated separately for each finite difference, with the assumed input concentration of biogas containing 40 % CO_2 and 60 % CH_4 .

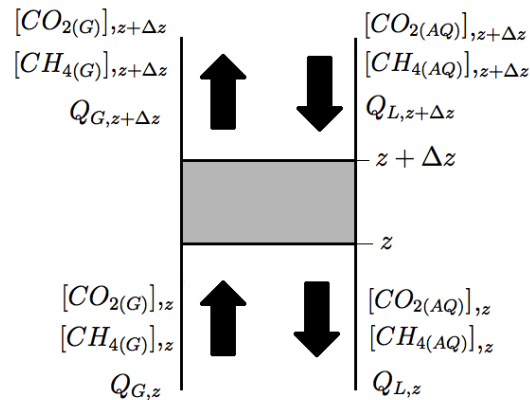


Figure 1: Differential element of absorption column. With z the position along the absorption column; Δz the height of the finite element, the gaseous and aqueous flow rates are shown by Q_G and Q_L , respectively, the concentrations for CO_2 in the gaseous and aqueous phase are shown by $[CO_{2(G)}]$, $[CO_{2(AQ)}]$, and similarly for CH_4 by $[CH_{4(G)}]$, $[CH_{4(AQ)}]$, respectively.

A plug flow model was assumed for the liquid and gas phases since the dispersion from turbulence and diffusion is expected to be low, as shown by Hiby¹⁰ and Therning and Rasmuson.¹¹ Equation 1 illustrates the steady state version of the model, with the accumulation

of the mass over time equal to zero. The flow rate from figure 1 is given by the product of the cross sectional area (A) and velocity (u).

$$A \frac{\partial c}{\partial t} = 0 = -A \frac{\partial c(u)}{\partial z} - N \quad (1)$$

The mass transfer flux (N) between the gas and liquid phases can be calculated from the overall mass transfer coefficient (K), the interfacial area (a) and the concentration driving force, as shown by equation 2. For the liquid side mass transfer the concentration driving force is defined as the difference between the concentration in the bulk phase of the liquid (c) and the dissolved concentration in equilibrium with the bulk phase of the gas (c_{eq}), which can be calculated using Henry's law.²⁰

$$N = Ka(c - c_{eq}) \quad (2)$$

This equation was applied to the gas and liquid phases of the CO_2 and CH_4 in the column using a forward finite difference to approximate the solution to equation 1. The liquid velocity (u_L) was assumed constant over the column height (z).

The overall mass transfer coefficient (K) can be calculated with the mass transfer resistance through both the gas ($1/k_G H_G$) and liquid films ($1/k_L$), as shown in equation 3 where H_G is the Henry's law constant. For both CO_2 and CH_4 the liquid side mass transfer resistance is dominant over the gas side mass transfer resistance.

$$\frac{1}{K} = \frac{1}{k_G H_G} + \frac{1}{k_L} \quad (3)$$

Many equations have been proposed to calculate the mass transfer coefficients for gas and liquid phases. Hottel et al.²¹ and Wang et al.⁹ list some of these for packed absorption columns. Equations suggested by Onda et al.,¹⁶ Billet and Schultes,¹⁷ Wagner et al.¹⁸ and Maćkowiak¹⁹ (shown in Table 1 along with equations for the effective interfacial area) were

used in this work. These four equations for the mass transfer coefficient are all based on Higbie's penetration theory, with the liquid side mass transfer coefficient proportional to the square root of the diffusivity. The correlation from Onda et al. was developed from literature data covering a range of liquids and experimental conditions. This remains one of the most widely used and successful expressions for the mass transfer coefficient in packed beds, although it may prove out of date for modern packing types. The more recent correlation from Billet and Schultes has been designed for counter-current absorption columns, but should be applicable to both random and structured packings; whereas the work from Wagner et al. is based on modern high efficiency random packings. The underlying hydrodynamics from Wagner et al. are based on work from Stichlmair et al.,²² which applies the theory of fluidized beds to packed beds. The resulting correlations for the liquid hold-up and pressure drop from Stichlmair et al. include packing constants which were derived from experimental results. The most recent correlation proposed by Maćkowiak uses a hydrodynamic model based on flow through channels and the Darcy-Weisbach equation for flow in pipes. This correlation is more suited to simpler packing types which are cylindrical or spherical in shape.

The pressure drop is also an important consideration in packed beds. For the gaseous phase the Ergun equation²³ was used to calculate the hydrodynamic pressure drop throughout the packed bed. The changes in the gas composition and mass as it passes through the column are considered in the model, although advection induced by the pressure drop is not taken into account. The largest contribution to the pressure drop, however, will be from the mass transfer of CO_2 from the gas phase which is absorbed into the liquid phase.

The Peng and Robinson equation of state has been incorporated into the model to take account of the departure from ideal gas behaviour at higher pressures. The constants and mixing rules for the CO_2 and CH_4 in biogas were taken from Peng and Robinson.²⁴

Energy Analysis

The main energy requirements of the water scrubbing process, as highlighted by Bauer et al.,⁴ are from pumping water (P_P), compressing biogas (P_C) and cooling the compressed gas (P_{COOL}). In this work the total power requirement (P_T) from these three processes has been calculated to analyse the overall energy requirement, as shown in equation 4.

$$P_T = P_P + P_C + P_{COOL} \quad (4)$$

The power requirement for pumping water (P_P) was calculated from the water density (ρ_L), gravitational acceleration (g) and liquid flow rate (Q_L) shown in equation 5. In this case, the mechanical efficiency of the pump (η_P) was assumed to be 60 %.

$$\frac{P_P}{\eta_P} = \rho_L g Q_L H_T \quad (5)$$

The total pressure head (H_T) was calculated as the sum of the pressure difference ($H_{COL} - H_{ATM}$), and the static (H_S) and dynamic (H_D) head as shown by equation 6. The static head was taken as the height of the absorption column, while the dynamic head was calculated from the Darcy Weisbach equation. Table 2 lists the assumed values used to calculate the dynamic head loss, with the Colebrook White equation used to calculate the friction factor. The pressure difference was taken as that between the atmospheric pressure and the pressure in the column; all pressure heads were expressed in m .

$$H_T = H_S + H_D + (H_{COL} - H_{ATM}) \quad (6)$$

To estimate the power requirement of the compressor, isentropic compression was assumed (equation 7). The number of compression stages (n) was set based on the input and output pressure (p_1 and p_2 , respectively), with an assumed maximum compression ratio of 4.3. The calculated pressure ratio was taken to be equal for each of the compression stages. The heat

capacity ratio of biogas (γ) was calculated from the heat capacity at constant pressure and at constant volume of CH_4 and CO_2 , depending on their respective concentrations in the biogas.

$$\frac{P_C}{\eta_C} = np_1 Q_G \left(\frac{p_2}{p_1} \right) \left(\frac{\gamma}{\gamma - 1} \right) \left(\frac{p_2}{p_1} \left(\frac{\gamma-1}{n\gamma} \right) - 1 \right) \quad (7)$$

The heat capacity values were taken from Poling et al.²⁰ An isentropic efficiency of 75 % was assumed for the gas compression, while the mechanical efficiency, which takes into account losses from the seals and valves in the compressor, was assumed to be 80 %.

Inter-cooling between the compression stages is required to reduce the high temperatures generated during compression: this was assumed to reduce the temperature of the compressed biogas to 10 K above ambient temperature. The temperature (T_2) after compression was calculated from equation 8, where the subscripts 1 and 2 denote the input and output, respectively. The flow rate of coolant (Q_{COOL}) required to cool the gas by a temperature difference $T_2 - T_1$ was calculated using the gas density (ρ_G) and specific heat of the gas (c_{PG}) with water as the coolant. The flow rate of water required in the heat exchanger was calculated from equation 9. The power requirement for cooling the biogas was then calculated from equation 5 using the flow rate of the coolant.

$$T_2 = T_1 \left(\frac{p_2}{p_1} \right)^{\left(\frac{\gamma-1}{\gamma} \right)} \quad (8)$$

$$Q_{COOL} = \frac{Q_G \rho_G \gamma_G (T_{G2} - T_{G1})}{\rho_L \gamma_L (T_{L2} - T_{L1})} \quad (9)$$

To reduce the quantity of CH_4 dissolved in the water a flash tank can be used downstream of the absorption column, to drop the pressure and encourage desorption of CH_4 . During this process a proportion of the dissolved CO_2 is also released, but the technique can drastically cut overall CH_4 losses from the system. In this work the flash tank was assumed to operate

at 2 bar and its performance was estimated by assuming equilibrium conditions. The energy inputs from the flash tank operation include the water pumping, and gas compression of the recaptured CH_4 and CO_2 to re-enter the absorption column.

The water from the absorption column can be regenerated by stripping the remaining dissolved CO_2 in a desorption column. This operates at low or atmospheric pressures and involves a counter-current air flow through random packing to maximise the contact surface area. The liquid flow rate is the same as that pumped through the absorption column; however, it is assumed that the desorption column operates under atmospheric pressure. The energy analysis includes the power requirement for the air blower and the water pump for the desorption step.

A 0.25 kW baseline power consumption for the control of valves and equipment was recorded during the pilot plant operation,²⁵ and this was therefore added to the simulated energy demand.

Experimental setup

The model developed was validated using both a pilot-scale and a full-scale gas upgrading plant. The pilot plant is based at the Centre for Rural Development and Technology, IIT Delhi, India and the full-scale operational plant in Tohana, Haryana, India. Both absorption columns are operated in counter-current mode, but have different geometries, work at different pressures and flow rates, and use different packing types. The pilot-scale experiments from IIT Delhi were conducted in a 3.0 m tall column filled with 15 mm metal Intalox random packing (IMTP). The column contained a mist eliminator to remove moisture from the outlet gas stream and a liquid distributor was located at the top of the column with a re-distributor placed half way up the column to ensure an even liquid distribution. The

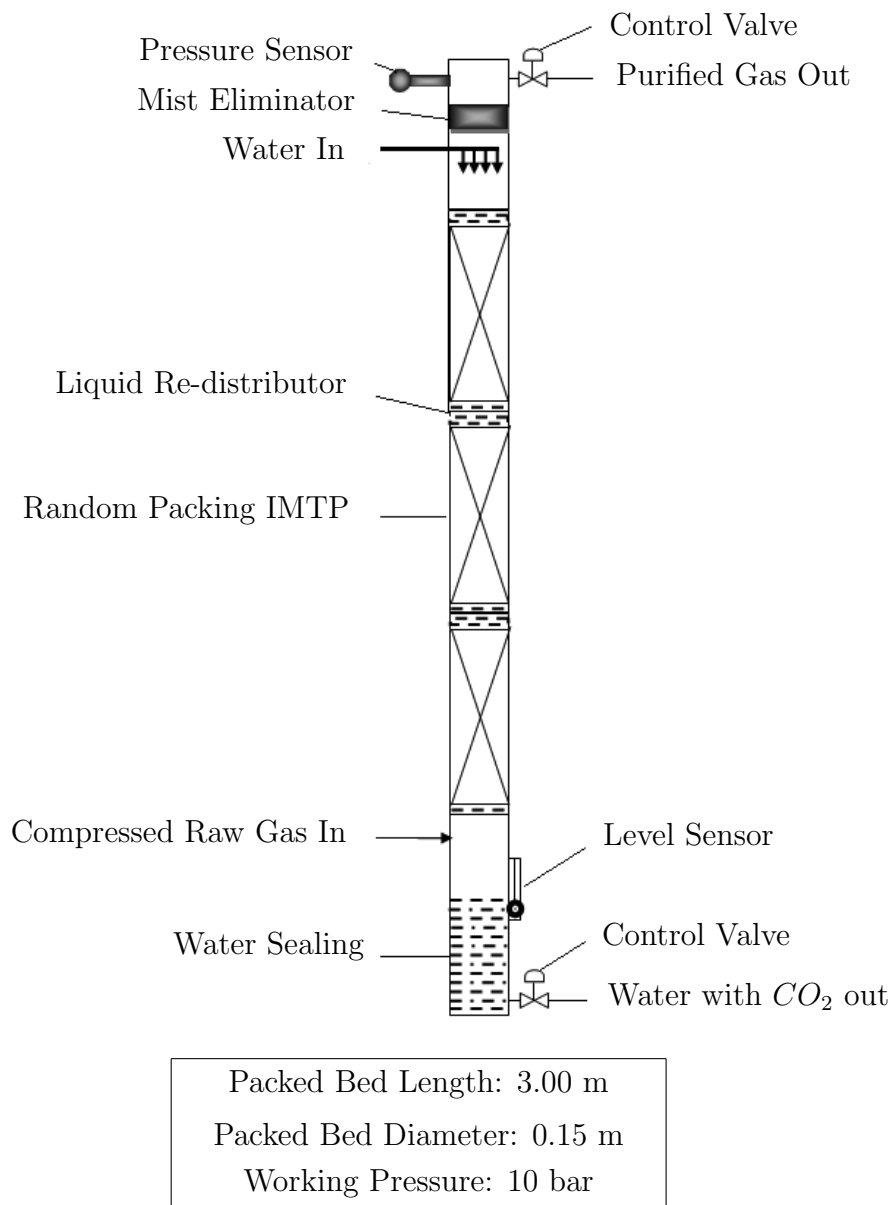


Figure 2: Schematic of pilot scale absorption column taken from Lântelä and Luostarinen²⁶

input biogas stream is compressed to 10 bar and fed from the base of the column. Figure 2 shows a schematic of the pilot plant set-up, taken from Lantela and Luostarinen.²⁶

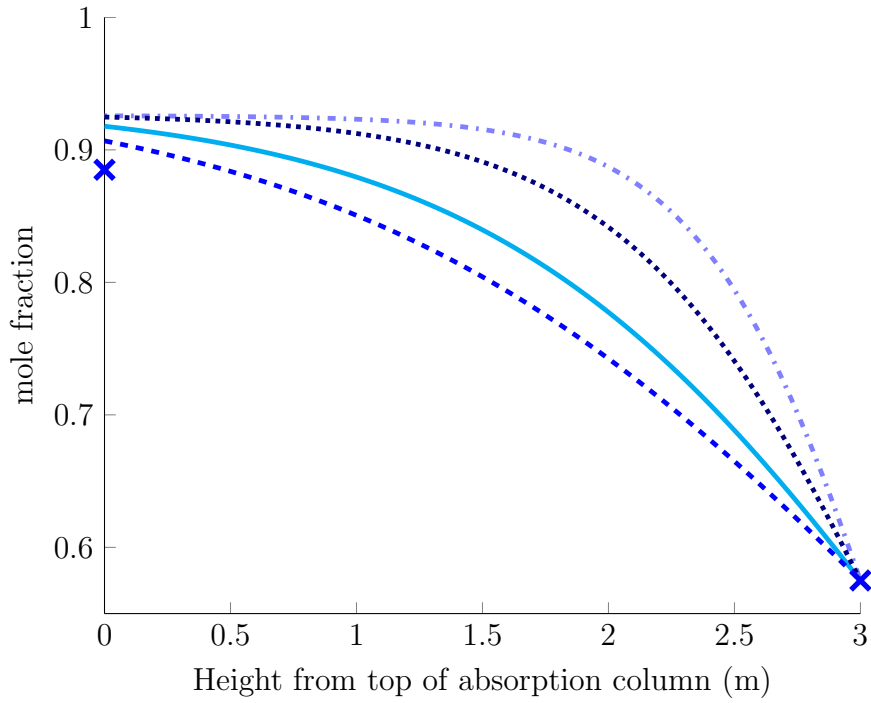
The full-scale operational plant in Tohana processes up to $60 \text{ m}^3 \text{ hr}^{-1}$ of biogas produced from the anaerobic digestion of cattle dung and local wastes. This upgrading unit does not operate at an elevated pressure, but instead relies on a large water flow rate to absorb the CO_2 . The ratio of gas flow rate to liquid flow rate is approximately 1:1, rather than the ratio of approximately 5:1 operated by the pilot plant. The upgrading unit is over 10 m tall and is filled with 25 mm plastic pall rings. Once upgraded the biogas is compressed into cylinders. Table 3 lists the specifications of the two absorption columns.²⁶

High liquid or gaseous velocities can result in the absorption column flooding, therefore the column diameter needs to be large enough to prevent this. The flooding limit developed by Billet and Schultes²⁷ was used in this model; with a recommended liquid design velocity between 70 - 80% of this limit.²⁷ In the case of the pilot-scale column the liquid velocity is high, with a consequent possibility of flooding.

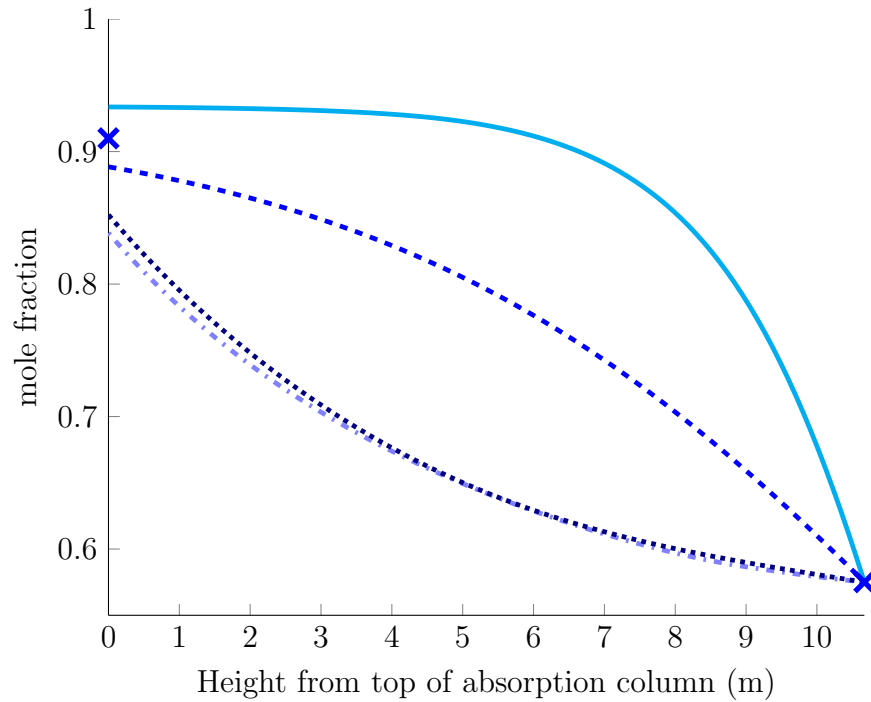
Results and discussion

Mass Transfer Coefficient Comparison

The rate-based mass transfer model was validated from the two absorption columns described in the experimental set-up section. The output from the four different mass transfer coefficient equations of Onda et al.,¹⁶ Wagner et al.,¹⁸ Maćkowiak¹⁹ and Billet and Schultes¹⁷ is shown in figure 3. Figure 3a compares the predicted CH_4 output concentrations for the pilot-scale plant, and figure 3b for the low pressure, large-scale absorption column in Tohana. The average output composition of biomethane from the pilot plant was 89% CH_4 and 5% CO_2 , with the remainder being air and water. In this model the mass transfer coefficient



(a) IIT Delhi pilot scale absorption column



(b) Large scale Tohana absorption column

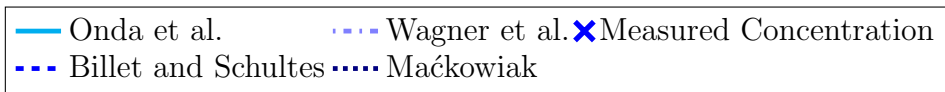


Figure 3: Comparison between mass transfer coefficients from literature and measured values

correlation from Billet and Schultes gave the closest approximation, with a predicted CH_4 output concentration of 90.7%. All of the relationships shown overestimated the CO_2 mass transfer, with the largest discrepancy being a CH_4 output concentration of 92.6% based on Wagner et al.

The Billet and Schultes equation also showed the closest match with the full-scale absorption column, with the predicted output CH_4 concentration of 88.9% slightly lower than the measured value of 91%. The other mass transfer coefficient equations showed a larger spread of results for the low pressure column than the pilot-scale column. In this case both the modern correlations from Wagner et al. and Maćkowiak under-predicted the mass transfer, while the correlation from Onda et al. slightly over-predicted the mass transfer.

Table 4 shows the pilot-scale experimental values and those predicted with the correlations from Wagner et al. and Maćkowiak. The interfacial areas calculated with these two equations are much larger than those from Onda et al. and Billet and Schultes. The equations of Wagner et al. and Maćkowiak are more sensitive to the superficial liquid velocity, which is particularly high for the case of the pilot plant. This resulted in a large liquid hold-up and for the case of Wagner et al. and Maćkowiak a large effective interfacial area.

Performance Index

A performance index (ξ) was used to quantify the efficiency of the CO_2 removal for the absorption process. The performance index is defined by equation 10 where y_r and y_e are the mole fractions of CO_2 in the raw and enriched biogas, respectively.

$$\xi = \left(\frac{1 - y_e/y_r}{1 - y_e/100} \right) \quad (10)$$

Figure 4 compares the performance index calculated with the mass transfer correlation from Billet and Schultes and the measured values from the pilot-scale absorption column. Throughout the experimentally tested range of liquid flow rates, the model shows good agreement with the measured values, with a calculated r^2 value of 61% between experimental and modeled results.

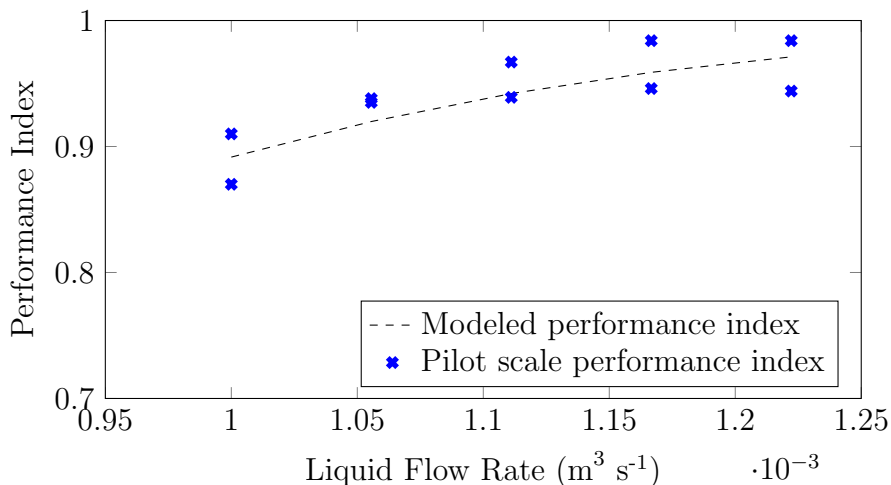


Figure 4: Performance index measured from pilot scale column and estimated from model

Sensitivity Analysis

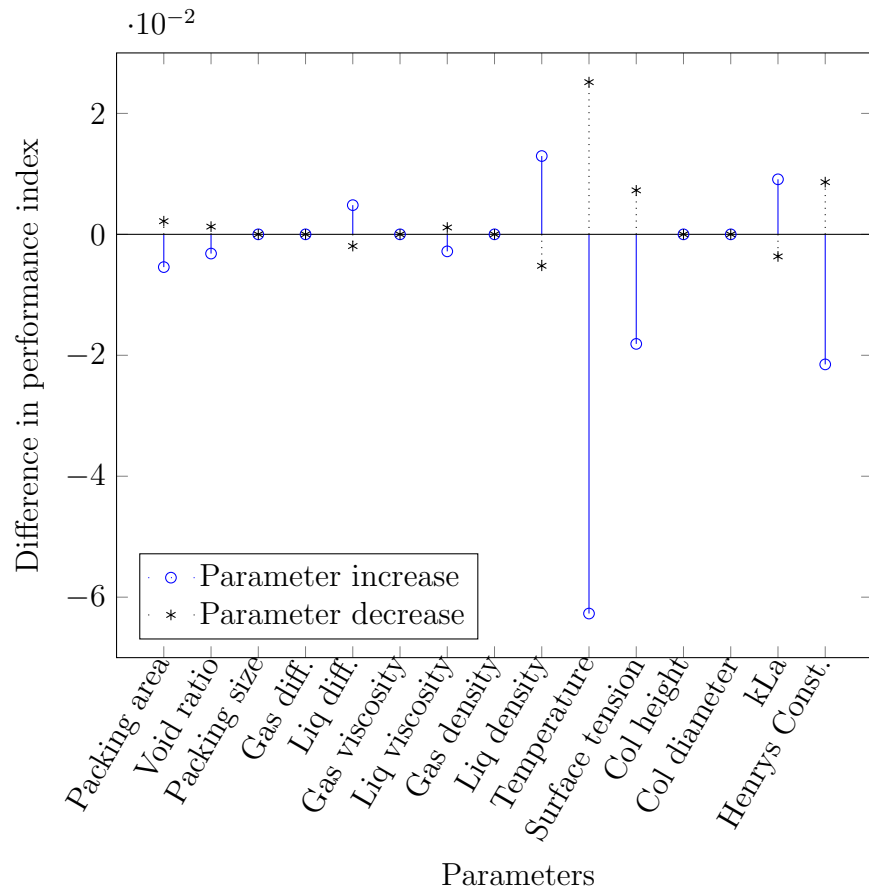
A sensitivity analysis was conducted to identify the relative importance of the model input parameters. Figure 5a shows the effect on the calculated performance index after changing each parameter by 10% from the values obtained using the Billet and Schultes equation. The temperature was altered by 10 K rather than 10%, but this has the largest effect on the performance index. An increase in temperature reduces the solubility of CO_2 in water, and thus reduces the concentration difference driving the mass transfer. The next most influential parameter on the performance of the absorption column is Henry's constant. The solubility of CO_2 as represented by Henry's constant is very sensitive to temperature change, i.e. at 293 K a 10 K temperature increase results in a 26% change in Henry's constant. The

temperature also affects several other parameters in the model, notably the diffusivity and viscosity of the biogas and water, although this has a minimal effect compared to the change in Henry's constant.

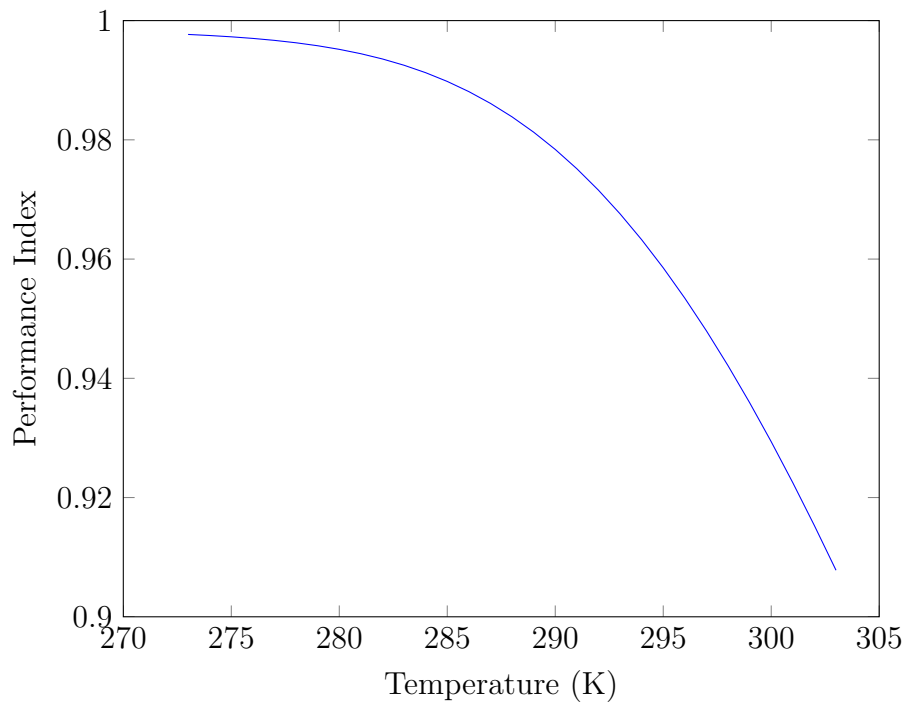
The implications of the ambient temperature and the effect this could have in upgrading biogas and capturing CO_2 in cooler conditions are further illustrated in figure 5b. The reduction in the CO_2 removal efficiency, shown by the performance index, is greater at higher temperatures. At ambient temperatures below 283 K the performance index is estimated by the model to be approximately 0.99. This reduces to 0.96 and 0.90 at 293 K and 303 K , respectively. With an input $CO_2 : CH_4$ ratio of 0.4 : 0.6, the temperature rise from 283 K to 293 K would correspond to a 1% reduction in CH_4 and a further 2% reduction between 293 K and 303 K .

As well as the temperature, the liquid density and surface tension also have noticeable influences on the performance index. An increase in density and reduction in surface tension improve the mass transfer. The liquid density is incorporated into all of the mass transfer coefficient correlations used in this work, and has a crucial role in calculating the liquid holdup and flooding limit; while the liquid surface tension is used in the correlation from Billet and Schultes to determine the wetted area of packing.

Interestingly, the correlations from Onda et al., Maćkowiak and Wagner et al. all showed significantly less sensitivity to the variation in the input parameters than the correlation from Billet and Schultes. The greatest influence on the performance index for all the correlations, however, was still from changes in temperature.



(a) Sensitivity analysis using correlation from Billet and Schultes¹⁷



(b) Effect of temperature on the performance index

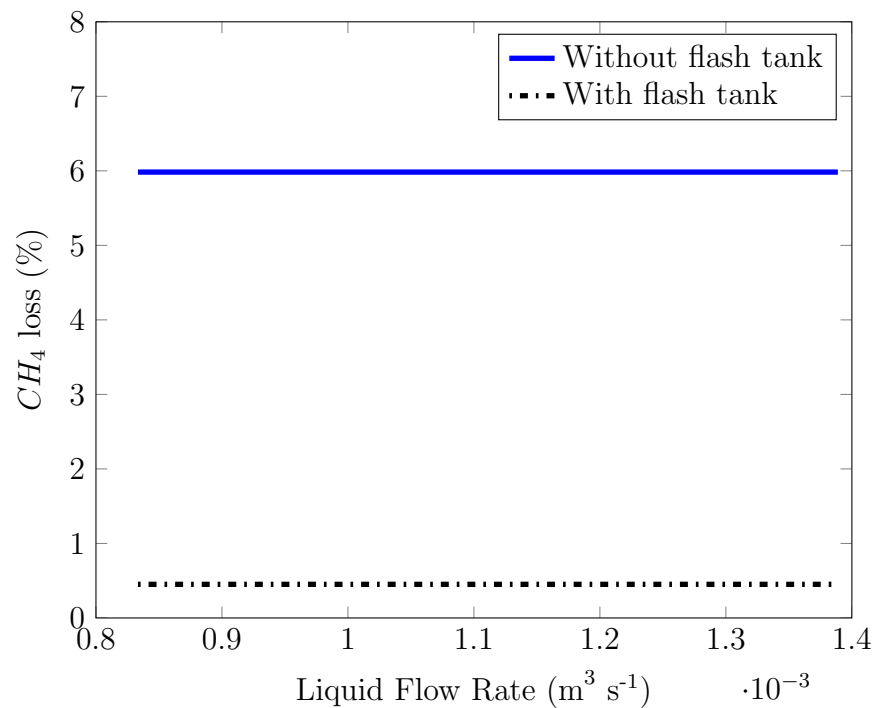
Figure 5: Sensitivity analysis and temperature effect on performance index

Methane losses

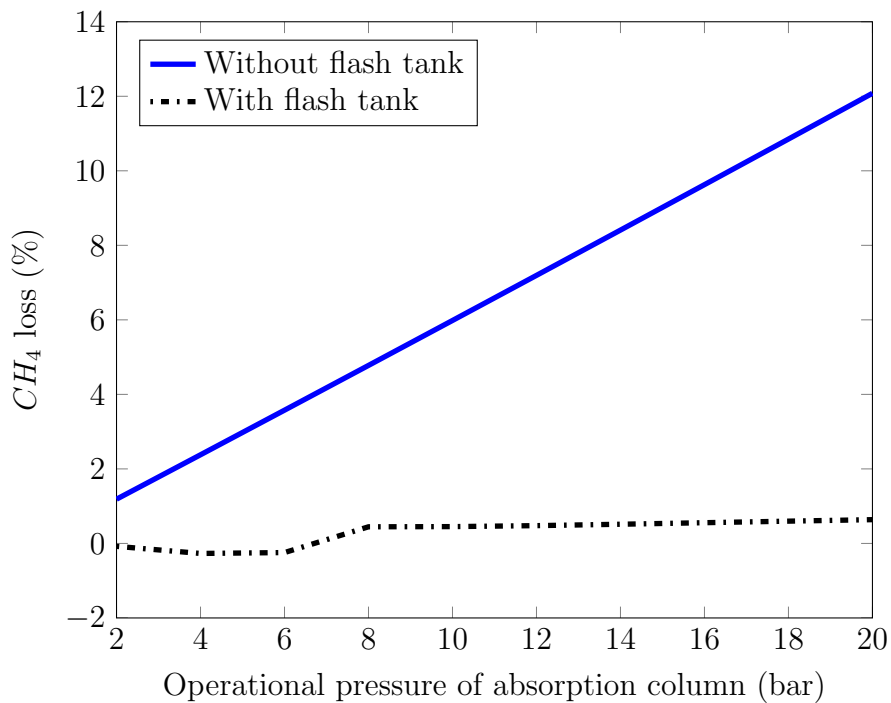
The pilot-scale plant employs a CH_4 recovery step, by treating the water exiting the absorption column in a flash tank where it is depressurised to approximately 2 bar. The large-scale absorption column at Tohana operates under a lower pressure and this CH_4 recovery step is not necessary. Figure 6a and 6b show the effect of the liquid flow rate and pressure on the potential CH_4 loss. Without a flash tank there can be substantial CH_4 losses, with 6% of input CH_4 absorbing in the water at a pressure of 10 bar. Reducing the pressure below 5 bar gives CH_4 losses of around 3 %, in which case a CH_4 recovery step may be less important for energy potential, although still desirable in terms of reducing greenhouse gas emissions. Persson⁸ reported up to 18 % CH_4 losses recorded in a water scrubbing plant working at a pressure of 20 bar. This was operating without a flash tank and the measurements were taken with a large margin of error. Persson reported that a flash tank would be expected to reduce CH_4 losses to under 2 %.

Energy Consumption

Table 5 compares the energy analysis from this work with the small number of studies previously reported in the literature. Persson and Berglund and Börjesson quote values for biogas upgrading in general, and do not specify whether these are based on the water scrubbing process. Smyth et al. gives a value for water scrubbing, although the pressure of the absorption column is not specified; while Jury et al. and Bauer et al. do not provide any information on the flow rates used. Improvements in the efficiency of the upgrading process should also be considered: the earlier work from Persson, Berglund and Börjesson quotes a higher energy demand than the more recent studies of Jury et al. and Bauer et al. The uncertainty surrounding the quoted energy requirements has resulted in a wide range of reported energy values. Despite this, the experimental and simulated energy requirements agree well with each other and fit within the range of values from the literature.



(a) CH_4 loss with increasing liquid flow rate, with pressure at 10 bar



(b) CH_4 loss with increasing pressure. Flash tank scenario assuming equilibrium conditions, liquid flow rate $1 \times 10^{-3} m^3 s^{-1}$

Figure 6: Simulated CH_4 loss from absorption column. Flash tank scenario assume equilibrium conditions

The literature values from Berglund and Börjesson and Jury et al. were quoted as a percentage of the energy content contained in the output biomethane and input biogas, respectively. For the purposes of converting this into kWh , the lower calorific value of CH_4 was taken as 32.8 MJ m^{-3} (at $298^\circ K$ and 101.325 kPa).²⁰ Using the above assumption the energy demand of the absorption column was modeled to require 4.2 % of the energy contained in the input raw biogas, compared to the measured value of 4.8 % in the pilot plant. This is not directly comparable, however, as the absorption column requires electrical energy, and the CH_4 contains chemical energy. There are high losses in conversion to electrical energy, but this approach can provide a useful check that the energy demands of the upgrading process are not greater than the energy contained in the biomethane. When making a full energetic and economic comparison the efficiency of conversion to useful energy, whether as electricity, heating, or vehicle fuel, should also be considered.

Figure 7a shows the effect of increasing the pressure in the absorption column on the energy requirement and liquid flow rate. From 4 bar the energy input of the absorption column increases with pressure. A significant proportion of the input energy is from the gas compression. As the pressure increases, the increase in energy requirement reduces, similar to the energy demand for a gas compressor. At a pressure of 2 bar, the liquid flow rate is high and consumes a high proportion of the energy demand. This is dramatically reduced when the pressure increases. With a gas flow rate of $20 \text{ m}^3 \text{ hr}^{-1}$ the pilot plant requires a water flow rate of $10.8 \text{ m}^3 \text{ hr}^{-1}$ to achieve a 90% CH_4 output at 2 bar pressure; at 4 bar this reduces to $6.1 \text{ m}^3 \text{ hr}^{-1}$ and at 8 bar this is $3.5 \text{ m}^3 \text{ hr}^{-1}$.

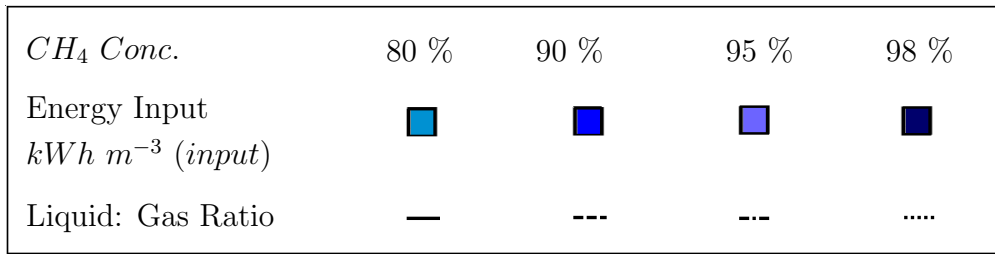
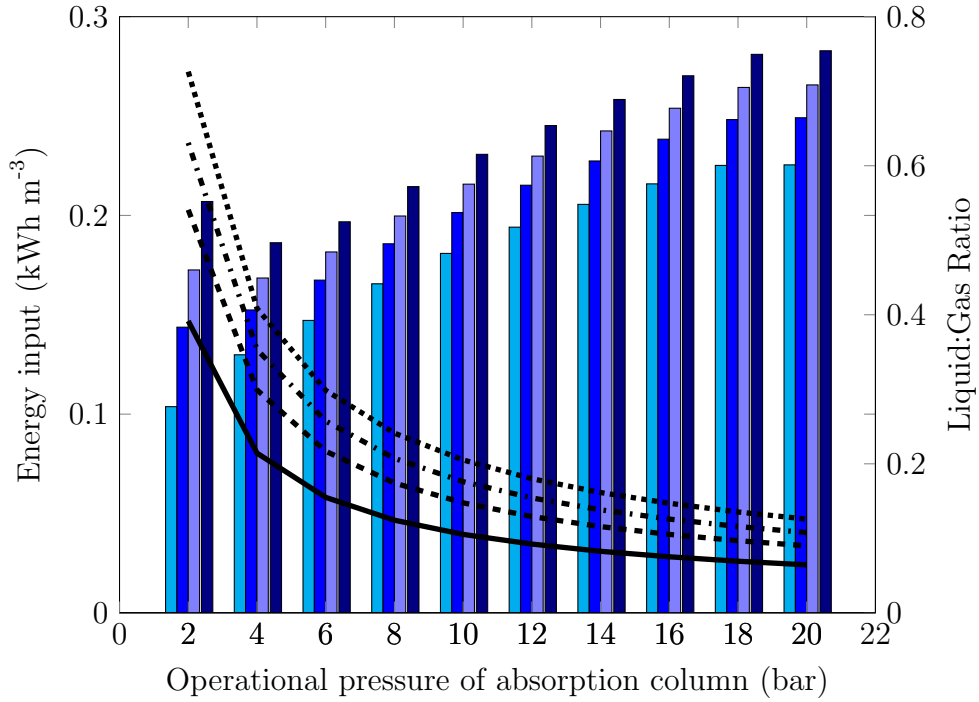
Figure 7b shows the calculated gas velocity loading limits for the range of superficial liquid velocities used in figure 7a. The superficial gas velocity in the pilot-scale absorption column is 0.032 m s^{-1} . Operating at 70% of the flooding limit²⁷ restricts the superficial liquid

velocity to approximately 0.02 m s^{-1} . With a column diameter of 0.3 m this results in a maximum liquid flow rate of $1.4 \times 10^{-3} \text{ m}^3 \text{ s}^{-1}$. The column diameter could be increased, similar to the low pressure absorption column in operation at Tohana. This would allow a greater liquid flow rate, but would also increase the capital costs.

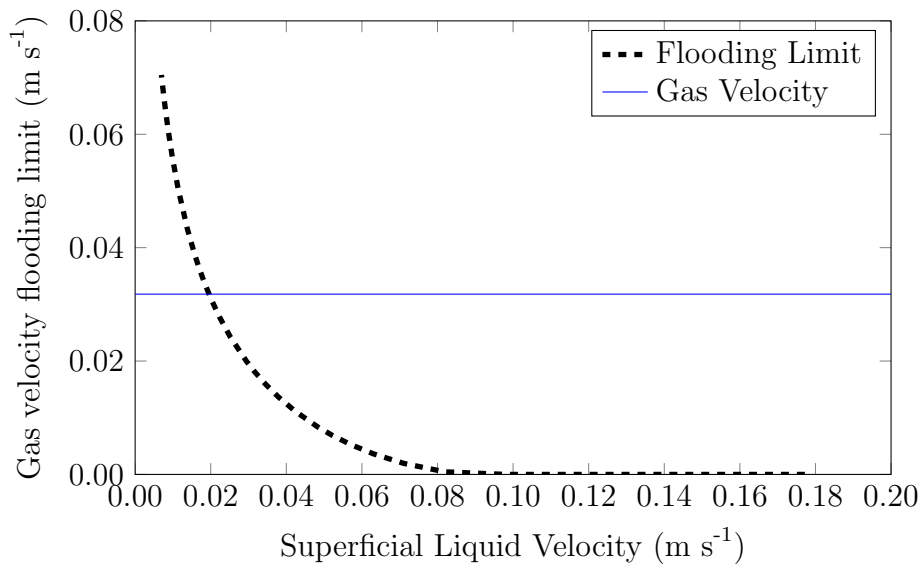
The energy requirement at the low pressure plant at Tohana with a gas flow rate of $50 \text{ m}^3 \text{ hour}^{-1}$ was estimated as 2.44 kWh Nm^{-3} , with the vast majority of this from pumping $75 \text{ m}^3 \text{ hour}^{-1}$ of water. This gave a CH_4 concentration of 92.5 %. This energy demand is an order of magnitude greater than that of the pilot-scale plant, indicating that operating under atmospheric pressure requires a substantially higher energy demand than operating at an increased pressure.

Depending on the resources available, and whether water regeneration will be employed, a compromise must be made between the energy usage and water requirement. To achieve 90% CH_4 purity with pressures under 10 bar a substantially larger quantity of water and a larger column would be required. If this water is readily available or can be recycled back into the absorption column then operating at a lower pressure is feasible. Recycling the water requires a CO_2 desorption step using a flash tank or desorption column, with an additional energy cost as shown in figure 8. The energy requirements of the flash tank and desorption column are approximately equal, as the main energy demand is from pumping the water, which is the same in both cases. Above 10 bar, the flash tank and desorption column consume only a very small fraction of the energy demand, due to the low water requirement at the higher pressure. When operating at a low pressure, the water demand is reduced when operating with a flash tank and desorption column, although the energy demand will increase, and below 4 bar this increase is dramatic.

If the biogas is to be compressed and stored at a high pressure after upgrading, it maybe



(a) Bar chart of energy requirement for absorption column and line chart for water requirement, results were simulated for the pilot plant with different solvent flow rates and biogas pressures to achieve stated output *CH₄* concentration



(b) Flooding limit for varying liquid flow rates in pilot scale column

Figure 7: Flooding limit for varying liquid flow rates in pilot scale column

beneficial to run the absorption column at a higher pressure. Figure 8 shows the energy consumption for compression of the biomethane to 200 bar. When this is included, operating the absorption column under lower pressure gives smaller energy savings. It must also be remembered that the capital and running costs for a column able to withstand a higher operating pressure will be higher.

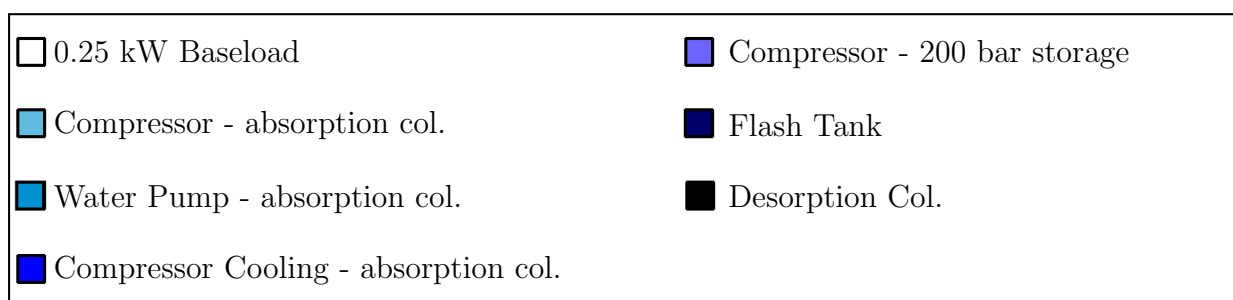
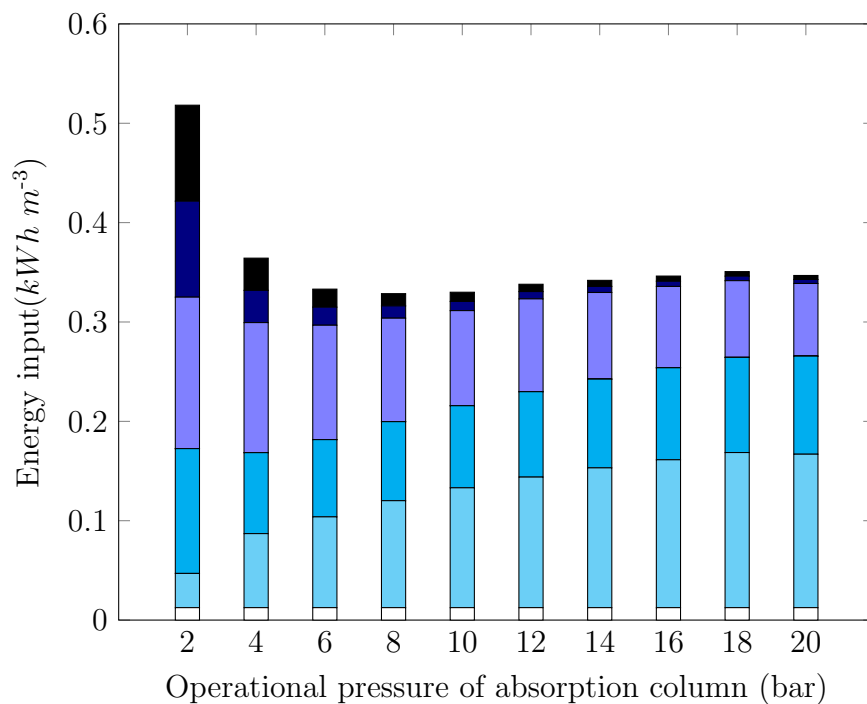


Figure 8: Energy requirement to achieve 95 % CH_4 , including CH_4 recovery, water regeneration and pressurisation for storage at 200 bar

Considering the absorption column only, operation at 4 bar had the lowest energy requirement to achieve a 95 % CH_4 concentration. When storage of biomethane is necessary and the energy demands of compression to 200 bar are included, operating the absorption column

at 6 bar gave the lowest energy demand. When CH_4 losses are recovered and the water is regenerated with a flash tank and desorption column, operating at 8 bar showed the lowest energy demand.

Similar results were found at different output CH_4 concentrations, although at 80 % CH_4 the energy demand for operation at reduced pressures is lower, as the water quantity is reduced. Above 20 bar there is a gradual increase in the total energy input. The lowest range in energy demand, including compression to 200 bar, is given by operating the absorption column between 6 - 10 bar. It should be remembered that the energy model in this work does not include all of the processes used to treat biogas before utilisation: many of these are dependent on the input biogas quality and the design specifications for the output biomethane, such as a pre-treatment to reduce the H_2S concentration, or a post-treatment to remove moisture. This model does, however, provide a detailed insight into the main processes that affect the energy demand in upgrading biogas by the water scrubbing technique.

Conclusion

A mass transfer rate-based model was developed to simulate and allow optimisation of the input parameters of an absorption column for upgrading biogas. The model was validated with data from two very different absorption columns. A sensitivity analysis highlighted the significance that the ambient temperature has on the absorption of CO_2 in water and on the performance of the absorption column. For the process to achieve a 98% CH_4 concentration an energy requirement of 0.23 kWh Nm^{-3} was required, this was slightly lower than the 0.26 kWh Nm^{-3} reported for the pilot plant, but is an improvement on values and estimates previously reported in literature. With CH_4 recovery and water regeneration the simulated energy requirements increase to 0.25 kWh Nm^{-3} , and with pressurisation to 200 bar this goes up to 0.35 kWh Nm^{-3} . The model can provide a useful tool in the design and techno-

economic analysis of CO_2 capture and biogas upgrading processes.

Acknowledgement

The authors acknowledge the EU FP7 VALORGAS project number 241334 and the support of Professor Charles Banks from the University of Southampton and Professor Virendra Vijay from IIT Delhi.

References

1. Salter, A.; Chu, T.; Heaven, S. *D 6.3 Output from an energy and carbon footprint model verified against primary data*; Public deliverable EU FP7 VALORGAS project (grant agreement no. 241334), 2013.
2. Kaparaju, P. *D 5.1 Evaluation of potential technologies an operational scales reflecting market needs for low-cost gas upgrading systems*; Public deliverable, EU FP7 VALORGAS project (grant agreement no. 241334), 2011.
3. Persson, M.; Jönsson, O.; Welliger, A. *Evaluation of Upgrading Techniques to Vehicle Fuel Standards and Grid Injection*; 2006.
4. Bauer, F.; Hulteberg, C.; Persson, T.; Tamm, D. *Biogas upgrading - Review of commercial technologies*; 2013.
5. Berglund, M.; Börjesson, P. Assessment of energy performance in the life-cycle of biogas production. *Biomass Bioenergy* **2006**, *30*, 254 – 266.
6. Smyth, B. M.; Murphy, J. D.; O'Brien, C. M. What is the energy balance of grass biomethane in Ireland and other temperate northern European climates. *Renewable and Sustainable Energy Reviews* **2009**, *13*, 2349 – 2360.

7. Jury, C.; Benetto, E.; Koster, D.; Schmitt, B.; Weltring, J. Life Cycle Assessment of biogas production by monofermentation of energy crops and injection into the natural gas grid. *Biomass and Bioenergy* **2010**, *34*, 54 – 66.
8. Persson, M. *Evaluation of upgrading techniques for biogas*; 2003.
9. Wang, G. Q.; Yuan, X. G.; Yu, K. T. Review of Mass-Transfer Correlations for Packed Columns. *Ind. Eng. Chem. Res.* **2005**, *44*, 8715–8729.
10. Hiby, J. W. *Longitudinal and transverse mixing during single-phase flow through granular beds*; 1962; pp 312–320.
11. Therning, P.; Rasmuson, A. Liquid dispersion and gas holdup in packed bubble columns at atmospheric pressure. *Chem. Eng. J.* **2001**, *81*, 69–81.
12. Gabrielsen, J.; Michelsen, M. L.; Stenby, E. H.; Kontogeorgis, G. M. Modeling of CO_2 Absorber Using an AMP Solution. *AIChE J.* **2006**, *52*, 3443–3451.
13. Yeh, J. T.; Pennline, H. W.; Resnik, K. P. Study of CO_2 Absorption and Desorption in a Packed Column. *Energy Fuels* **2001**, *15*, 274–278.
14. Rao, A. B.; Rubin, E. S. A technical, economic, and environmental assessment of amine-based CO_2 capture technology for power plant greenhouse gas control. *Environ. Sci. Technol.* **2002**, *36*, 4467–75.
15. Rasi, S.; Läntelä, J.; Veijanen, A.; Rintala, J. Landfill gas upgrading with countercurrent water wash. *Waste Manage.* **2008**, *28*, 1528 – 1534.
16. Onda, K.; Takeuchi, H.; Okumoto, Y. Mass transfer coefficients between gas and liquid phases in packed columns. *J. Chem. Eng. Jpn.* **1968**,
17. Billet, R.; Schultes, M. Predicting Mass Transfer in Packed Columns. *Chem. Eng. Technol.* **1993**, *77*, 1 – 9.

18. Wagner, I.; Stichlmair, J.; Fair, J. R. Mass Transfer in Beds of Modern, High-Efficiency Random Packings. *Ind. Eng. Chem. Res.* **1997**, *36*, 227–237.
19. Maćkowiak, J. Model for the prediction of liquid phase mass transfer of random packed columns for gas/liquid systems. *Chem. Eng. Res. Des.* **2011**, *89*, 1308 – 1320.
20. Poling, B.; Thomson, G. H.; Friend, D. G.; Rowley, R. L.; Wilding, W. V. In *Perry's Chemical Engineers' Handbook*, 8th ed.; Perry, R., Green, D., Eds.; McGraw Hill: New York, 2008; Chapter 2.
21. Hottel, H.; Noble, J. J.; Sarofim, A.; Silconx, G. D.; Wankat, P. C.; Knaebel, K. S. In *Perry's Chemical Engineers' Handbook*, 8th ed.; Perry, R., Green, D., Eds.; McGraw Hill: New York, 2008; Chapter 5.
22. Stichlmair, J.; Bravo, J.; Fair, J. General model for prediction of pressure drop and capacity of countercurrent gas/liquid packed columns. *Gas Sep. Purif.* **1989**, *3*, 19 – 28.
23. Macdonald, I. F.; El-Sayed, M. S.; Mow, K.; Dullien, F. A. L. Flow through Porous Media-the Ergun Equation Revisited. *Ind. Eng. Chem. Fundamen.* **1979**, *18*, 199–208.
24. Peng, D.; Robinson, D. B. A New Two-Constant Equation of State. *Ind. Eng. Chem. Fundamen.* **1976**, *15*, 59–64.
25. Kapoor, R.; Vijay, V. *D 5.2 Evaluation of existing low cost gas bottling systems for vehicles use adaption in developing economies*; Public deliverable EU FP7 VALORGAS project (grant agreement no. 241334), 2013.
26. Läntelä, J.; Luostarinen, J. *D 5.4 Results of design, construction and testing of low-cost modular biogas upgrading systems*; Confidential deliverable, EU FP7 VALORGAS project (grant agreement no. 241334), 2013.
27. Billet, R.; Schultes, M. Prediction of Mass Transfer Columns with Dumped and Arranged

Packings: Updated Summary of the Calculation Method of Billet and Schultes. *Chem. Eng. Res. Des.* **1999**, *77*, 498 – 504.

Graphical TOC Entry

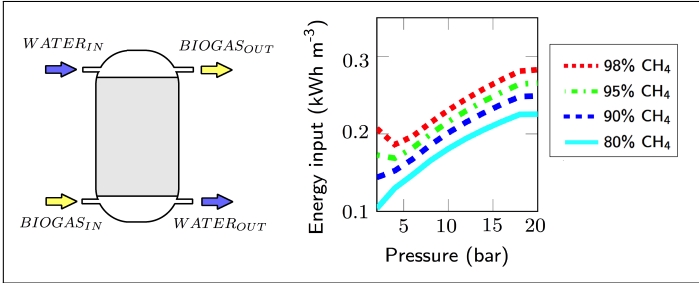


Table 1: Equations showing calculation for the mass transfer coefficients and effective interfacial area. Parameters defined as per nomenclature

Correlation	Reference
$k_G = 5.23 \left(\frac{a_p D_G}{RT} \right) \left(\frac{\rho_G u_G}{a_p \mu_G} \right)^{0.7} Sc_G^{(1/3)} (a_p d_p)^{-2}$ $k_L = 0.0051 (a_p d_p)^{0.4} \left(\frac{\rho_L g}{\mu_L} \right)^{(1/3)} (Re_L)^{(2/3)} Sc_L^{(-1/2)}$ $a_W/a_p = 1 - \exp[-1.45 (\sigma_c/\sigma)^{0.75}] (Re_L^{0.1}) (Fr_L^{-0.05}) (We_L^{0.2})$	Onda et al. ¹⁶
$k_G = C_G \frac{a_p^{0.5} D_G}{\sqrt{d_h(\epsilon-h_L)}} \left(\frac{\rho_G u_G}{a_p \mu_G} \right)^{3/4} Sc_G^{(1/3)}$ $k_L = C_L \left(\frac{\rho_L g}{\mu_L} \right)^{(1/6)} \left(\frac{D_L}{d_H} \right)^{(0.5)} \left(\frac{u_L}{a_p} \right)^{(1/3)}$ $a_W/a_p = 1.5 (a_p d_H)^{-0.5} Re_L^{-0.2} We_L^{0.75} Fr_L^{-0.45}$	Billet and Schultes ¹⁷
$k_G = \sqrt{\frac{4\Phi_G D_G u_G}{\pi(\epsilon-h)zC_{PK}^2}}$ $k_L = \sqrt{\frac{4\Phi_L D_L u_L}{\pi h z C_{PK}^2}}$ $a_W/a_P = \left[\left(\frac{1-\epsilon+h}{1-\epsilon} \right) - 1 \right]$	Wagner et al. ¹⁸
<p><i>For $Re_L < 2$</i></p> $k_L = \frac{3.842 D_L^{1/2} u_L^{1/3}}{(1-\phi_P)^{1/3} d_H^{1/4} (3/g)^{1/6} a_p^{1/3} \nu_L^{1/6}}$ $a_W = 6.49 a_p^{2/3} \frac{\Delta\rho^{1/2} g^{1/6} \nu_L^{1/3} u_L^{1/3}}{\sigma_L^{1/2}}$ <p><i>For $Re_L > 2$</i></p> $k_L = \frac{5.524}{\sqrt{\pi}} \frac{a_p^{1/12} D_L^{1/2} g^{1/6} u_L^{1/6}}{(1-\phi_P)^{1/3} \epsilon^{1/4}}$ $a_W/a_P = 3.42 Fr_L^{1/3} \left(\frac{We}{Fr_L} \right)^{1/2}$	Maćkowiak ¹⁹

Table 2: Assumptions for calculating the energy requirement of the absorption column

Variable	Value
Pump efficiency	60%
Isentropic efficiency	75%
Compressor mechanical efficiency	80%
Water pipe diameter	0.02 m
Water pipe length	5.0 m + column height
Head loss from water pipe bends	3.0 m
Colebrook White pipe friction factor	0.3

Table 3: Overview of pilot-scale IIT Delhi and large-scale Tohana absorption columns used to validate model, taken from Lantela and Luostarinen²⁶

	Pilot Scale Plant IIT Delhi	Operational Plant Tohana
Column height (m)	3.00	10.67
Column diameter (m)	0.15	0.90
Biogas flow rate ($m^3 hr^{-1}$)	20	60
Liquid flow rate ($m^3 hr^{-1}$)	3.6 - 4.4	65 - 75
Packing type	15 mm IMTP	25 mm Plastic Pall rings
Input CH_4 (Volume %)	55 - 60	56 - 59
Input CO_2 (Volume %)	35 - 40	34 - 40
Output CH_4 (Volume %)	89 - 95	90 - 92
Output CO_2 (Volume %)	3 - 7	3 - 7

Table 4: Modeled molar fraction of CO_2 and CH_4 using the mass transfer coefficient expressions from Onda et al.,¹⁶ Billet and Schultes,¹⁷ Wagner et al.¹⁸ and Maćkowiak¹⁹ for the pilot scale absorption column

	$k_L CH_4$	$k_L CO_2$	α ($m^2 m^{-3}$)	Output CH_4 (%)	Output CO_2 (%)
Onda et al. ¹⁶	2.97×10^{-4}	3.06×10^{-4}	205	91.8	1.1
Billet and Schultes ¹⁷	1.83×10^{-4}	1.89×10^{-4}	154	90.7	2.2
Wagner et al. ¹⁸	2.19×10^{-4}	2.26×10^{-4}	914	92.6	0.2
Maćkowiak ¹⁹	2.37×10^{-4}	2.45×10^{-4}	664	92.5	0.3

Table 5: Comparison of this work with reported literature values for the energy requirements of water scrubbing ($kWh\ m^{-3}$ (input)).

Reference	Conditions	Quoted Value	Energy requirement ($kWh\ m^{-3}$ (input))
Persson ⁸	General value for all biogas upgrading techniques	0.30 – 0.60 $kWh\ Nm^{-3}$ output biomethane	0.48 – 0.95 $kWh\ Nm^{-3}$ input biogas
Berglund and Börjesson ⁵	General value for all biogas upgrading techniques	11 % of energy content in output biomethane	0.60 $kWh\ Nm^{-3}$ input biogas *
Smyth et al. ⁶	Water scrubbing, pressure not specified	0.35 $kWh\ Nm^{-3}$ output biomethane	0.55 $kWh\ Nm^{-3}$ input biogas
Jury et al. ⁷	Water scrubbing, operating pressure: 8 bar	3% of energy content in raw, input biogas	0.16 $kWh\ Nm^{-3}$ input biogas *
Bauer et al. ⁴	Water scrubbing, operating pressure: 6 – 8 bar	0.35 $kWh\ Nm^{-3}$ input biogas	0.35 $kWh\ Nm^{-3}$ input biogas
Pilot scale experiment	Water scrubbing, 10 bar pressure, 96 – 97% CH_4	0.26 $kWh\ Nm^{-3}$ input biogas	0.26 $kWh\ Nm^{-3}$ input biogas
Modelled simulation	Water scrubbing, 10 bar pressure, 98 % CH_4	0.23 $kWh\ Nm^{-3}$ input biogas	0.23 $kWh\ Nm^{-3}$ input biogas

* Assumed lower calorific value for CH_4 of $32.8\ MJ\ m^{-3}$,²⁰ biogas input CH_4 concentration of 60 % and biomethane output concentration 95 %.